

# IBM Research Report

## Porosity Characterization by Beam-Based Three-Photon Positron Annihilation Spectroscopy

**Mihail P. Petkov, Marc H. Weber, Kelvin G. Lynn**

Dept. of Physics  
Washington State Univ.  
Pullman, WA 99164-2814

**Kenneth P. Rodbell**

IBM T. J. Watson Research Center  
P. O. Box 218  
Yorktown Heights, NY 10598



**Research Division**

**Almaden - Austin - Beijing - Haifa - T. J. Watson - Tokyo - Zurich**

# **Porosity characterization by beam-based three-photon positron annihilation spectroscopy**

Mihail P. Petkov, Marc H. Weber, and Kelvin G. Lynn

*Dept. of Physics, Washington State University, Pullman, WA 99164-2814*

Kenneth P. Rodbell

*IBM T. J. Watson Research Center, P.O. Box 218, Yorktown Heights, NY 10598*

June 25, 2001

We present a straightforward and fast positron annihilation spectroscopy (PAS) technique for measuring the two-to-three photon annihilation ratio of Ps (electron-positron) atoms ( $3\gamma$  PAS), utilized here for the non-destructive characterization of mesoporous (pore size  $> 1$  nm) dielectric films. Examples are given for  $\sim 1$   $\mu\text{m}$ -thick foamed MSSQ films, produced by mixing MSSQ (0–90 wt. % fraction) with a sacrificial foaming agent (porogen). Probing these films as a function of depth allows one to monitor Ps escape from interconnected pores. This Ps escape data is, subsequently, used to determine the threshold for pore interconnectivity to the film surface, which occurs prior to critical percolation. A classical treatment of Ps diffusion is used to calculate the open and closed porosity fractions as a function of the initial porogen load.

Porous materials have recently attracted the interest of the semiconductor industry, which seeks a suitable material for use as an interlayer dielectric (ILD) in microelectronic devices. The ever-increasing drive to improve the performance of modern devices is illustrated in the guidelines given by the *International Technology Roadmap for Semiconductors*.<sup>1</sup> Reduction of both the signal propagation delay and cross talk between neighboring metal wires can be achieved by using ILD materials with a low dielectric constant (low- $k$ ). A large variety of materials are presently being evaluated; however, a general consensus exists that regardless of the chemical composition, embedded pores ( $k \approx 1.0$  for air) will be required to lower the dielectric constant below approximately  $k = 2.2$ . A successful low- $k$  candidate must satisfy a set of mechanical and electrical requirements, many of which are strongly dependent on film porosity. Therefore, detailed knowledge of the porosity fraction, pore size distribution, pore interconnectivity and morphology, is required. In this letter positron annihilation spectroscopy (PAS) is used to measure the porosity in porous low- $k$  thin films.

PAS has been shown to be an accurate pore characterization tool for bulk polymers<sup>2,3</sup> and, recently, has been used to characterize porosity in thin ( $< 1 \mu\text{m}$  thick) films.<sup>4-10</sup> For mesoporous (pore size  $> 1 \text{ nm}$ ) dielectrics, PAS relies on the formation of Ps (a hydrogen-like positron-electron bound state), which can form either at a pore surface or in the solid and, subsequently, escape into a pore. Ps is attracted to pores, where it lowers its zero-point energy; the excess kinetic energy is subsequently lost through inelastic collisions with pore walls by molecular or lattice vibrations. Ps is thus confined to the pore after the first few interactions. The annihilation signature of *ortho*-Ps (*o*-Ps), the triplet Ps state with parallel orientation of the positron and electron spins,

depends on the pore size and shape. For *o*-Ps self-annihilation (the positron with its bound electron) at least 3 photons ( $3\gamma$ ) are required to conserve total momentum. This is a slow process, resulting in a  $\sim 142$  ns *o*-Ps lifetime in vacuum. In pores, however, Ps may undergo a “pick-off” annihilation event – with a molecular electron from the pore walls, having an opposite spin to that of the positron. Such events result in the emission of two photons ( $2\gamma$ ) and shorten the *o*-Ps lifetime (the annihilation rate of a positron and an electron with the opposite spin is  $>1000$  times higher than for a similar event with parallel spins). The probability of a pick-off annihilation event in large pores ( $> 1$  nm) depends on the collision rate with the pore walls or pore environments, and, therefore, on the pore size (and shape). For all practical purposes, Ps is assumed to thermalize within a negligible fraction of its lifetime in solids, and thus the pick-off rate is determined by the pore size, shape, and chemistry of the solid.

Positron annihilation lifetime spectroscopy (PALS) studies<sup>4-6</sup> take advantage of the *o*-Ps lifetime – pore size correlation models<sup>4,5,11</sup> to derive pore size distribution(s) from the distribution of the measured *o*-Ps lifetimes (inverse pick-off rates). The pick-off process also influences the ratio of  $2\gamma$  to  $3\gamma$  annihilation events. This can be used to derive porosity properties through measurements of the *o*-Ps self-annihilation ( $3\gamma$ ).

In this letter, we report a simple and fast method for characterizing the porosity in mesoporous films in terms of pore interconnectivity, percolation, and fraction of open porosity. This is accomplished using  $3\gamma$  PAS in conjunction with a variable energy positron beam that allows for depth profiling.

Thin ( $\sim 0.75$   $\mu\text{m}$ ) low- $k$  mesoporous MSSQ films, produced at IBM Almaden Research Center using a sacrificial polymer (porogen) technique,<sup>12</sup> were investigated. A

solution, containing low molecular weight MSSQ resin and porogen with variable weight fraction (0 – 90 wt. %), was spun on to Si/SiO<sub>2</sub> wafers. The blend was cured in a 300 Torr N<sub>2</sub> ambient in two steps, achieving first the vitrification of the MSSQ network (200 °C), and subsequently, the decomposition and evacuation of the volatile porogen (450 °C) forming pores within the MSSQ film.

A variable energy positron beam with a rate of  $2 \times 10^5$  e<sup>+</sup>/s was used to profile the films as a function of depth. The empirical relation between the mean positron implantation depth,  $\bar{z}$ , and the beam energy,  $E$  is  $\bar{z}(\text{nm}) = (40/\rho) \times E^{1.6}$  (keV),<sup>13</sup> where  $\rho$  (g/cm<sup>3</sup>) is the film density. At each selected beam energy, the  $\gamma$ -spectra with  $10^6$  events were acquired with a high-efficiency Ge detector. The *o*-Ps ( $3\gamma$ ) self-annihilation was parameterized by the  $3\gamma$ -to- $2\gamma$  annihilation ratio, calculated as  $(T-P)/P$ ,<sup>13</sup> where  $T$  is the total spectrum counts, and  $P$  is the number of integrated counts in the photopeak region (511±9 keV). Sufficient precision in the determination of the  $3\gamma$ -to- $2\gamma$  ratio can be achieved in 10's of seconds, which makes this an efficient method. The  $3\gamma$ -to- $2\gamma$  ratio was calibrated to measure the *o*-Ps fraction using Ps formation on the surface of a hot Ge crystal;<sup>14,15</sup> an *o*-Ps fraction of 100% indicates that all injected positrons form Ps.

Typical experimental  $3\gamma$  depth-profiles are shown in Figure 1 (top) to illustrate the effect of increasing (0-90 wt. %) porogen load. In the bottom plot, we use the data for the 40 wt. % sample as an example to illustrate features of these profiles from which the porosity properties are determined. The data are shown for  $\bar{z} < 0.4$   $\mu\text{m}$ , for which the influence of the substrate is negligible. The fit (thick solid line), based on Ref. [16], accounts for Ps formation (dashed line) and a diffusion-like Ps motion in the film (thin solid line); both components are shown extrapolated for a “bulk” (e.g., infinitely thick)

sample. The Ps formation reaches a plateau at shallow depths; that is, at low incident positron energies. (This is consistent with the available data for other polymers.<sup>17)</sup> Of greater interest to this work is the second component of the fit (“escape curve”), which in Ref. [16] describes Ps diffusion in a solid, through which Ps escapes to vacuum. Here, an analogy is drawn for Ps in mesoporous thin films, which escapes to vacuum from the pores.

The possibility of Ps escape (light atom diffusion) from open pores is high, since within its average lifetime Ps traverses a path length orders of magnitude larger than the film thickness. In vacuum, the  $3\gamma$  process is the only available annihilation channel, whereas for a given film, the balance between  $3\gamma$  and  $2\gamma$  events is set by the pore size and pore density. Hence, the asymptotic (“bulk”) level of the escape curve is related to the closed porosity. Further, the  $3\gamma$ -signal at each depth is a superposition of vacuum- and “bulk”-annihilation events, whose respective contributions depend on the ability of the Ps to reach the surface (and escape). Thus, the curvature of the escape curve defines a characteristic length for Ps escape from a given film, which we define here as the *Ps escape length*, or  $L_{esc}$ . This length is similar to molecular or atomic diffusion in pores; however, the decay lifetime is that of *o*-Ps.

For PAS, Ps escape to vacuum defines open porosity; i.e., open porosity is determined by the classical permeability of the probed material to atomic Ps gas. It is worth mentioning, that quantum mechanical effects (e.g., movement of Ps through “bottlenecks” between pores and/or tunneling through thin pore walls) are not taken into account here. Open porosity can be sealed in by a capping layer, however, the Ps interaction with this cap must also be considered. Ps interacts on the order of one

million times with the MSSQ walls prior to annihilation, whilst a single encounter with a metal cap will likely result in its annihilation. Other capping materials (non metals) may yield intermediate results depending on the interaction of the Ps with the layer. Thus a cap layer on an otherwise open porosity sample can complicate the Ps annihilation signatures (in both  $3\gamma$  and PALS).

The Ps escape length,  $L_{esc}$ , can be determined by using standard software for data analysis,<sup>18</sup> based on a diffusion model, which accounts for the shape of the positron implantation profiles at each implantation energy. Care has been taken to model the film/substrate interface, which acts as an absorbing boundary due to the efficient Ps pick-off at the lower MSSQ / SiO<sub>2</sub> interface. Ps annihilation at this interface is important only for highly porous samples, where  $L_{esc}$  becomes comparable with the film thickness. We extract from the  $3\gamma$ -profiles (Figure 1) the equivalent of a diffusion length,  $L$ .  $L$  is a measure of the length-scale over which two related processes occur: (1) positron/Ps diffusion in the solid and (2) Ps escape from open pores. For a variety of organic and inorganic solids, the Ps diffusion length is  $\sim 1$  nm,<sup>19</sup> and its contribution to  $L$  (10-1000 nm) is within the errors of the model. The positron diffusion length ( $L_+$ ) in all of these films, calculated from Doppler broadening data (as in Ref. [20]; data not shown here), was approximately 10 nm. Therefore,  $L_+$  is less important for large values of  $L$ , and  $L \approx L_{esc}$ . Taking advantage of the similar positron ( $\sim 2$  ns<sup>-1</sup>) and Ps annihilation rates ( $\sim 2.03$  ns<sup>-1</sup>, averaged over the *p*-Ps and *o*-Ps states),  $L^2 = L_{esc}^2 + L_+^2$  overestimates the contribution from positron diffusion when  $L$  is small ( $L \approx L_+$ ). Figure 2 shows the results for porogen loads less than 50 wt. %. Above  $\sim 25$  wt. % porogen load (inset),  $L_{esc}$  increases more rapidly with porogen load. We identify this critical porogen load value as

the *pore connectivity threshold*, above which pore clusters become connected to the surface on a finite scale. The percolation threshold, at which an infinite cluster (or continuous path through the film) is formed, lies at still higher porogen loads. For homogeneous and isotropically distributed pore clusters the value of  $L_{esc}$  is a measure of pore connectivity. In general, this method is sensitive to the surface normal direction.

The fractions of open and closed porosities in a film can be estimated from the “bulk”  $3\gamma$ -asymptotic level of the escape curve (i.e., see Figure 1, bottom). The  $3\gamma$ -contribution from the solid MSSQ matrix (which amounts to 2.6%), weighted with the respective fraction in the MSSQ-porogen mix, was subtracted from the calculated<sup>18</sup> value for each film. The resulting differences,  $\Delta 3\gamma$ , shown in Figure 3a represent the large (>1 nm) pores. Data for porogen loads greater than 60 wt. % were omitted, because of the significant loss of fast Ps (hot atom diffusion) into vacuum (through continuous percolation pathways to the film surface and substrate) which resulted in both decreased detector efficiency as well as enhanced Ps annihilation at the lower MSSQ / SiO<sub>2</sub> interface). Suppressed Ps formation in highly porous samples also contributes to the loss of Ps signal.

For isolated, fixed-size pores, the  $3\gamma$ -signal is proportional to the pore density and, therefore, the porogen load. Small variations in the pore size<sup>21</sup> results in marginal deviation from the linear relation between the  $3\gamma$ -signal and the porogen load. Thus one may assume a linear dependence for closed porosity (Figure 3a, line, porogen load  $\leq 25$  wt. %). When extrapolated to larger porogen loads, a sharp departure from closed porosity, and the onset of open porosity as observed by Ps, is evident.



Using this linear dependence for closed porosity ( $3\gamma$ -signal), evaluation of open and closed porosities as a fraction of the total porosity is straightforward. The measured experimental  $3\gamma$ -signal,  $\Delta 3\gamma_{exp}$ , is a superposition of the Ps signals from (1) closed pores,  $\Delta 3\gamma_{bulk}$ , and (2) Ps that has escaped to vacuum, which annihilates via  $3\gamma$  only (e.g.,  $3\gamma = 100\%$ ). Further, the fraction of escaped Ps is equated to the open porosity fraction. Quantum mechanical effects, such as transmission through narrow openings and tunneling through thin walls, are ignored, and Ps is treated classically. This is consistent with the short Ps diffusion lengths in polymers.<sup>19</sup> As a result, the open porosity fraction (Figure 3b),  $F_{open}$  ( $F_{open} + F_{closed} = 1$ ) is given by:

$$F_{open} = (\Delta 3\gamma_{exp} - \Delta 3\gamma_{bulk}) / (1 - \Delta 3\gamma_{bulk}) \cdot 100\% .$$

It is worth noting that the pore interconnectivity threshold (Figure 2) and the onset for open porosity (Figure 3b), which are obtained independently (curvature vs. asymptotic level of the escape curve), are in agreement.

In conclusion, we have demonstrated the feasibility of applying a simple  $3\gamma$  PAS technique for the characterization of  $\mu\text{m}$ -thick, mesoporous low-k dielectric films. Porosity characterization depth-profiles can be acquired in  $< 10$  min and could be performed more quickly with other detector arrangements. The length-scale describing Ps motion in a film was used to detect pore connectivity, from which the maximum porogen load resulting in the formation of isolated pores (pore interconnectivity threshold) was determined. Ps escape from the films was treated classically in order to calculate both the open and closed porosity fractions as a function of the initial porogen load.

## **Acknowledgements**

We would like to thank W. Volksen and R. D. Miller (IBM, Almaden Res. Ctr.) for fabricating the samples and for valuable discussions. This research was sponsored by the U.S. National Institute of Standards and Technology (NIST / ATP Cooperative Agreement No. 70NANB8H4013), by the IBM T.J. Watson Research Center [Research Partnership Award (K.G.L.)], and by the DOE Basic Energy Sciences.

## REFERENCES

1. Semiconductor Res. Corp., *International Technology Roadmap for Semiconductors 1999*.
2. Y.C. Jean, *Mater. Sci. Forum*, **175-178**, 59 (1995).
3. H. Yang and Y.C. Jean, *Mater. Sci. Forum*, **255-257**, 41 (1997).
4. D.W. Gidley, W.E. Frieze, T.L. Dull, A.F. Yee, E.T. Ryan, and H.-M. Ho, *Phys. Rev. B*, **60**, R5157 (1999).
5. D.W. Gidley, W.E. Frieze, T.L. Dull, J. Sun, A.F. Yee, C.V. Nguyen, and D.Y. Yoon, *Appl. Phys. Lett.*, **76**, 1282 (2000).
6. M.P. Petkov, M.H. Weber, K.G. Lynn, and K.P. Rodbell, *Appl. Phys. Lett.*, **77**, 2470 (2000).
7. Th. Gessmann, M.P. Petkov, M.H. Weber, K.G. Lynn, K.P. Rodbell, P. Asoka-Kumar, W. Stoeffl, and R.H. Howell, *Mater. Sci. Forum.*, **363-365**, 585 (2001).
8. M.P. Petkov, M.H. Weber, K.G. Lynn, K.P. Rodbell, W. Volksen, and R.D. Miller, *Advanced Metallization Conference*, San Diego, October 3-5, 2000, *in press (MRS Symp. Proc.)*
9. A. Uedono, Z.Q. Chen, R. Suzuki, T. Ohdaira, T. Mikado, S. Fukui, A. Shiota, and S. Kimura, submitted to *J. Appl. Phys.* (2001).
10. K.P. Rodbell, M.P. Petkov, M.H. Weber, K.G. Lynn, W. Volksen, and R.D. Miller, *Mater. Sci. Forum.*, **363-365**, 15 (2001).
11. K. Ito, H. Nakanishi, and Y. Ujihira, *J. Phys. Chem. B*, **103**, 4555 (1999).
12. C.J. Hawker, J.L. Hedrick, R.D. Miller, and W. Volksen, *MRS Bulletin*, **25**, 54 (2000).

13. P.J. Schultz and K.G. Lynn, *Rev. Mod. Phys.*, **60**, 701 (1988).
14. A.P. Mills, Jr., *Phys. Rev. Lett.*, **41**, 1828 (1978).
15. E. Soininen, A. Schwab, and K.G. Lynn, *Phys. Rev. B*, **43**, 10051 (1991).
16. M. Eldrup, A. Vehanen, P.J. Schultz, and K.G. Lynn, *Phys. Rev. B*, **32**, 7048 (1985).
17. L. Xie, G.B. DeMagio, W.E Freeze, G.W. Gidley, H.A. Hristov, and A.F. Yee, *Phys. Rev. Lett.*, **74**, 4947 (1995).
18. A. van Veen, H. Schut, J. de Vries, R.A. Hakvoort, and M.R. IJpma, in *Positron Beams for Solids and Surfaces*, London, Ont. Canada, ed. by P.J. Schultz, G.R. Massoumi, and P.J. Simpson, (AIP New York, 1990), p.171.
19. K. Hirata, Y. Kobayashi, and Y. Ujihira, *J. Chem. Soc. Faraday Trans.*, **92**, 985 (1996).
20. M.P. Petkov, M.H. Weber, K.G. Lynn, K.P. Rodbell, and S.A. Cohen, *J. Appl. Phys.*, **86**, 3104 (1999).
21. Small variations in the mean pore size as a function of porogen load was deduced from small angle X-ray scattering experiments.

## FIGURE CAPTIONS

**Figure 1.** Top: Examples of experimental  $3\gamma$  depth-profiles for MSSQ films with varying porogen loads. Bottom: A fit (thick line) using a simple model to illustrate the relevant information after accounting for Ps formation (dashed line). The thin solid line describes Ps atomic diffusion from connected pores into vacuum. The curvature of this thin line defines the Ps escape length, which is a measure of pore connectivity.

**Figure 2.** Ps escape length,  $L_{esc}$ , as a function of porogen load; the inset shows the low-porosity range. The crossing point of the lines (inset) identifies the pore interconnectivity threshold at  $\sim 25$  wt. %.

**Figure 3.** **(a)** The characteristic “bulk”  $3\gamma$ -signal, originating from the large ( $> 1$  nm) pores, as a function of porogen load. The linear fit to the  $\leq 25$  wt. % data represents the limit of closed cell porosity in these films. **(b)** The open porosity fraction,  $F_{open}$ , as a function of porogen load.

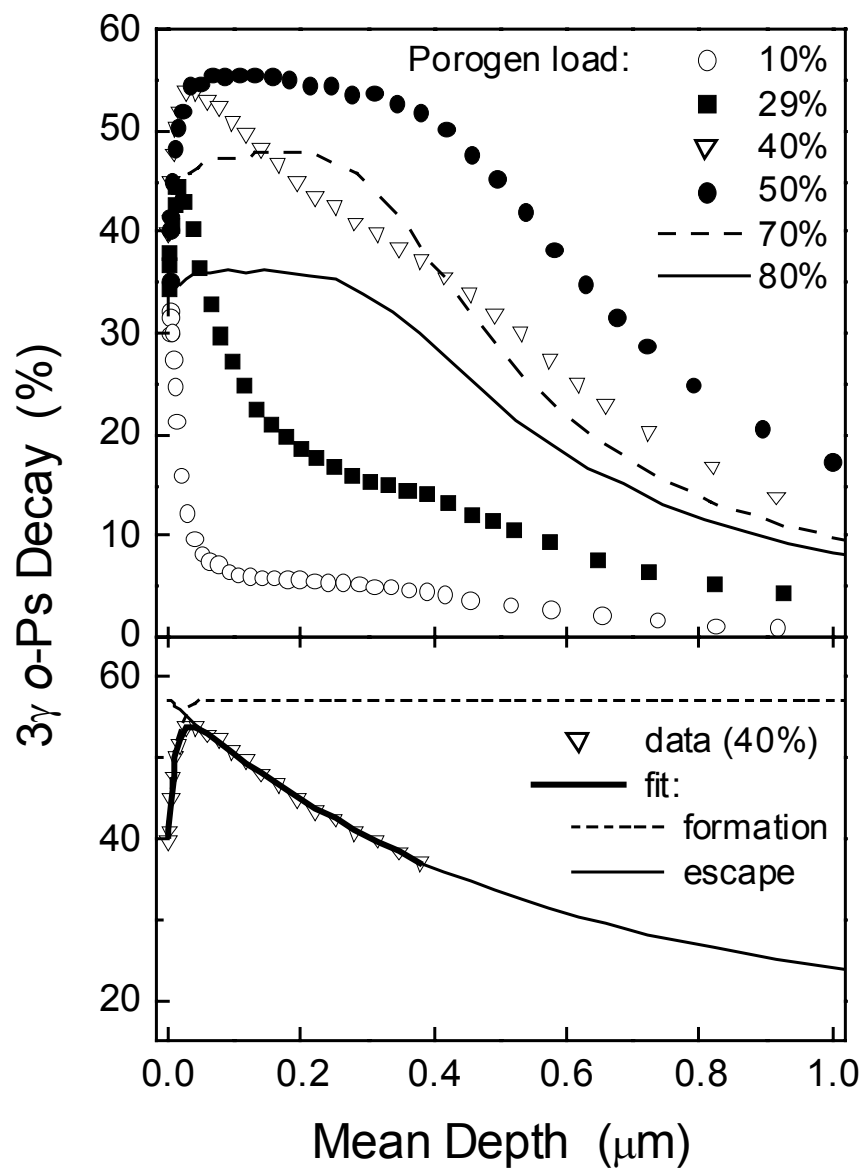


Figure 1 / 3 M. Petkov et al., APL

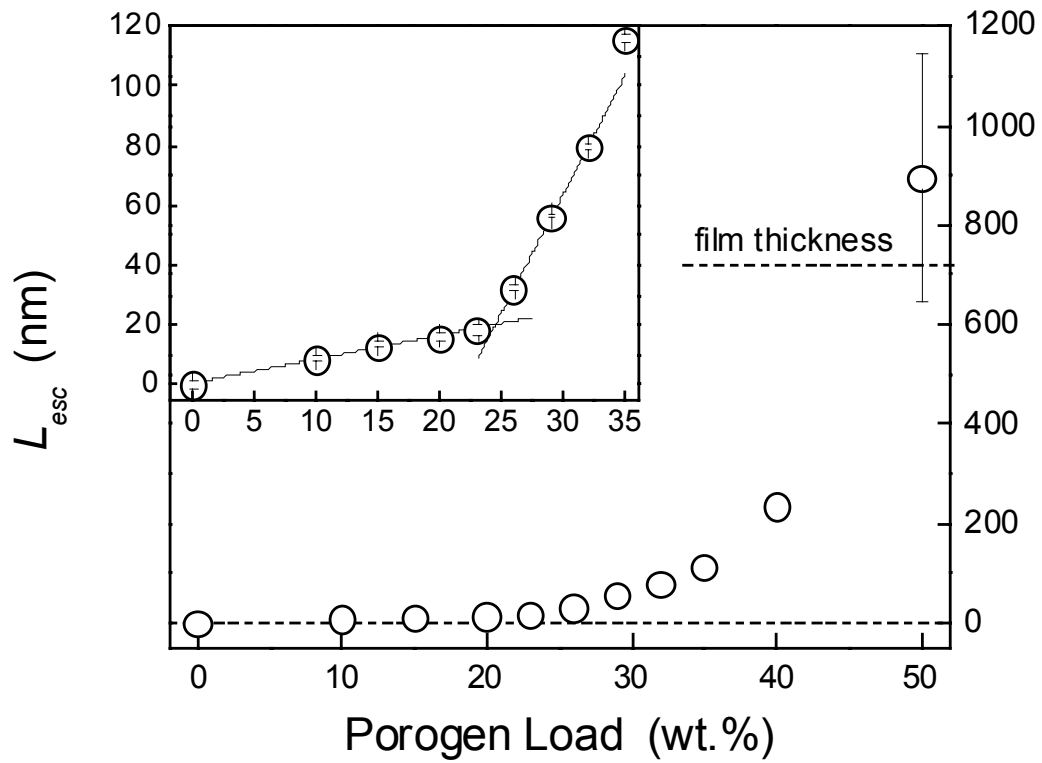


Figure 2 / 3 M. Petkov et al., APL

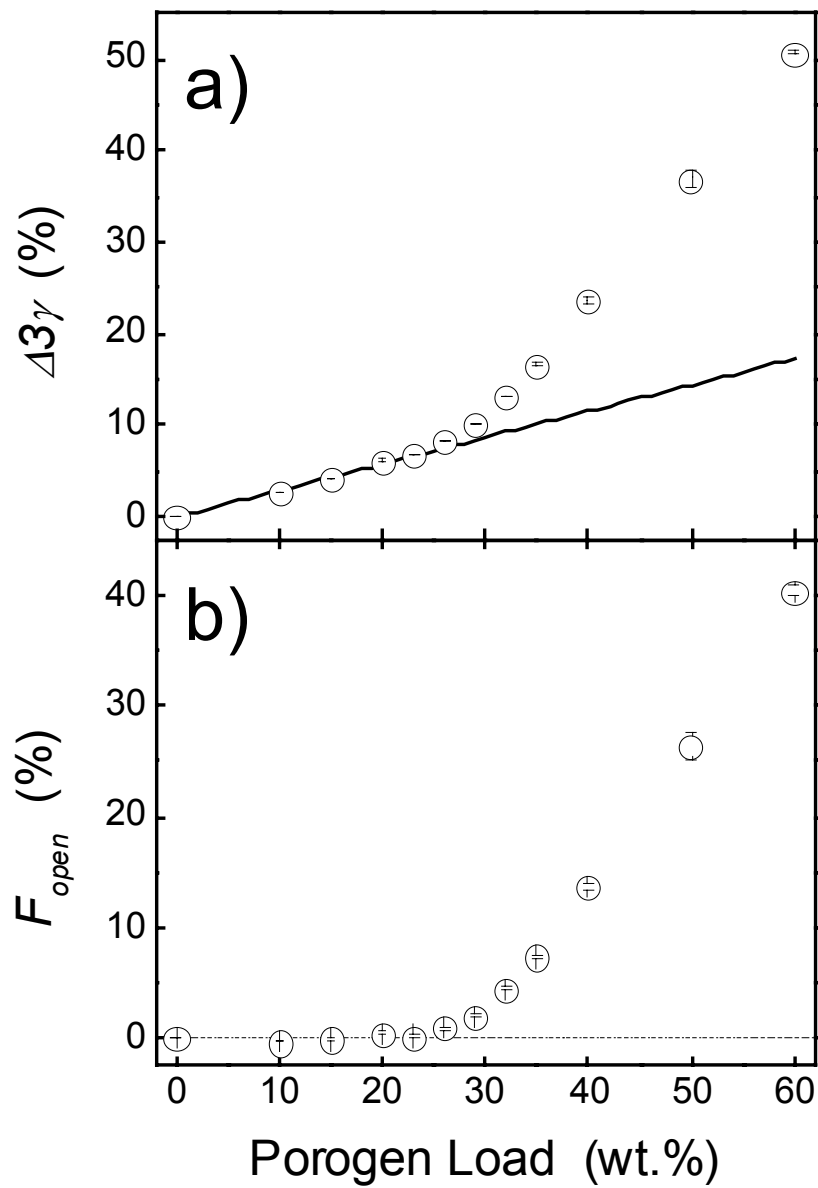


Figure 2 / 3 M. Petkov et al., APL